Chapter 3
Research methodology and finite element modelling

3.1 Introduction

This chapter summarizes the study's research methodology and brief layout of the experimental plan to achieve the set objectives. The whole study is divided into four different steps. The first step deals with viscoelastic material characterization of asphalt mixes, in which time and temperature dependency of the material is evaluated using creep compliance test. These creep compliance data were further converted to stress relaxation modulus. Generalized Kelvin model was further used to evaluate Prony series coefficients to be used as an input parameter in FE model of asphalt pavement. The second step characterizes unbound granular materials (UGMs) based on resilient modulus test. Resilient modulus of UGMs were determined using repeated load triaxial compression testing and various models were used to explain stress dependency of these materials.

The third step involves finite element (FE) modelling of tire-pavement system. A three-dimensional FE model of asphalt concrete pavement has been developed in this study using ABAQUS. The conventional geometric design consists of four different layers namely, bituminous concrete (including dense bituminous macadam), base layer, granular subbase layer, and compacted soil subgrade layer. Solid tire has been modelled to consider realistic nonuniform contact stress distribution at tire-pavement interface. It is easy to evaluate the material properties of solid tire as it consists of single rubber material. For modelling tire rubber, the suitable hyper-elastic material model was obtained using relevant tensile test data and a curve fitting approach [168]. Hyper-elastic models are

generally used to calculate elastomer's properties that respond elastically when subjected to large deformations [169].

The final step involves evaluation of the structural response of the asphalt pavement under different conditions. The idea of study is to analyze the usefulness of the FE model of tire-pavement system to (a) incorporate complex material properties of pavement layers (b) consider nonuniform stress distribution in loading area, and (c) explore structural response of the pavement under different conditions. The developed FE model after validation is used to calculate horizontal tensile strain at the bottom of the asphalt layer and vertical compressive strain at the top of the subgrade layer. These strains are further used to compute pavement life in rutting and fatigue. The flowchart of the research methodology is shown in Figure 3.1 and Figure 3.2.

Step I: Linear viscoelastic material characterization of asphalt mixes (Figure 3.2)

Step II: Nonlinear stress dependent material characterization of unbound granular materials in base, subbase, and subgrade layer (Figure 3.3)

Step III: Finite element modelling of tire-pavement system (Figure 3.4)

Step IV: Evaluation of structural response of asphalt pavement under different conditions

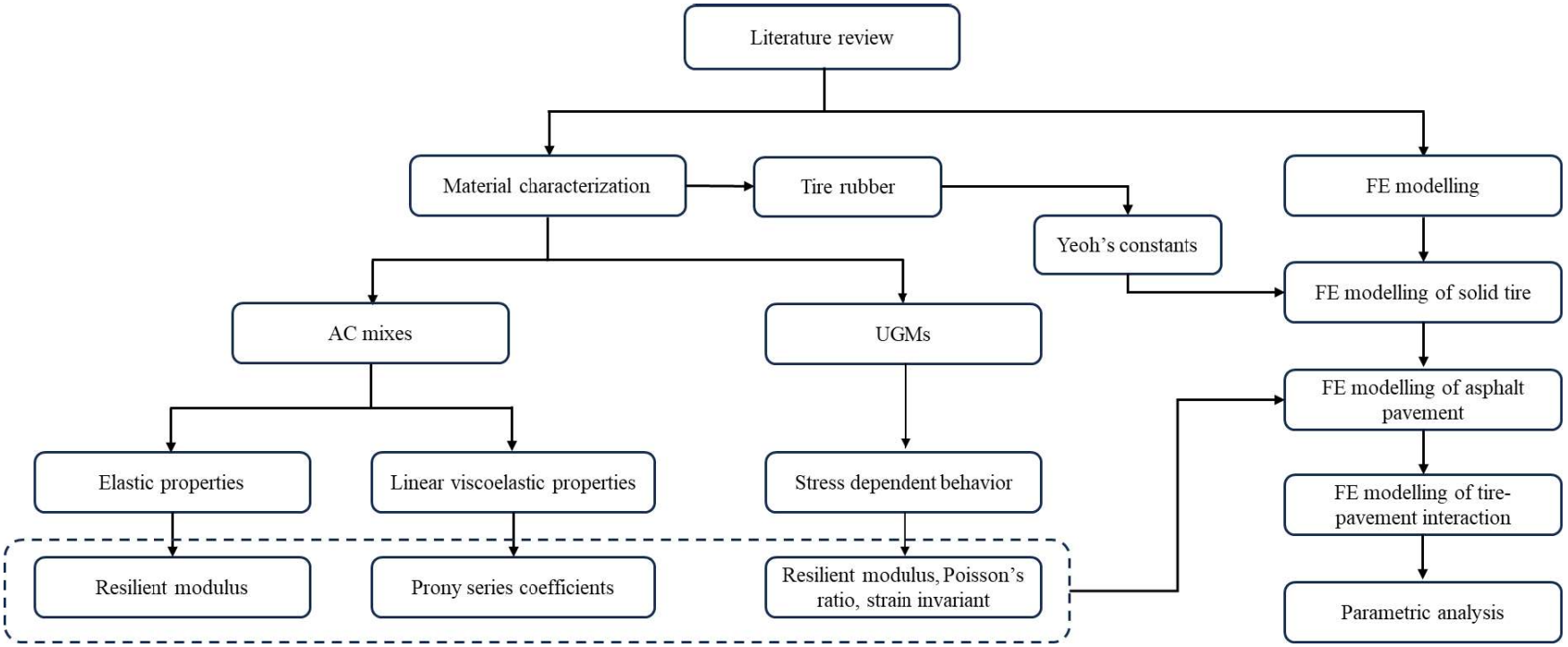

Figure 3.1. Flowchart of the research methodology.

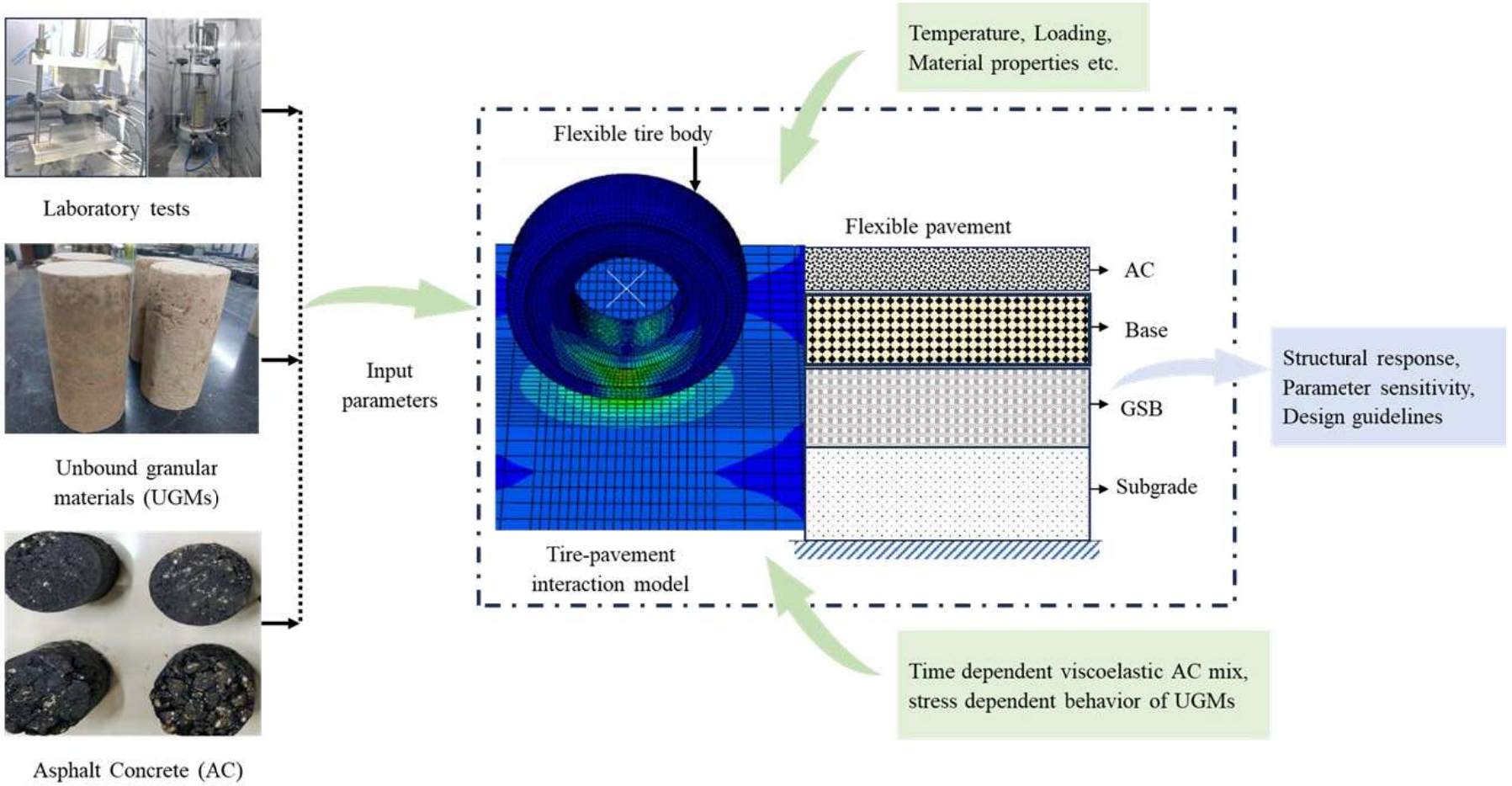

Figure 3.2. Pictorial representation of research methodology.

3.2 Step I: Linear viscoelastic material characterization of asphalt mixes

The first step emphasizes viscoelastic material characterization of AC mixes. The characterization of viscoelastic properties is often done by measuring creep behaviour [88]. The creep-related tests are popular because these tests make it possible to determine and separate the time-independent (elastic strain) and time-dependent (viscoelastic) components of the strain response [89] in a simplified way. In addition, parameters obtained from creep tests at low temperatures (m-value) are used to predict thermal cracking development and propagation, and those at high temperatures are used to predict rutting in the HMA [90].

As explained earlier, since asphalt mixes exhibits viscoelastic behaviour, controlling and conducting experiments for all different types of combinations to represent field conditions is nearly impossible. In such cases, analytical and computational tools are readily used. Increasing computational capabilities have allowed pavement scientists to study complex material behaviour using tools like finite element (FE), discrete element (DE), etc. [78]. To include viscoelastic characteristics in such tools, often a generalised Kelvin viscoelastic model (GKM) or Prony series model [99][97] is used.

State-of-the-art equipment such as dynamic modulus test, bending beam rheometer test, and creep compliance test is recommended to be used in developed nations. However, in developing nations, often limited resources are available and therefore conducting different types of tests is not always possible. In such cases, a simple test is required to obtain the desired behaviour. Creep compliance test facility is readily available in most of the research institutions. Creep compliance test measures material deformation with time at different temperatures which is defined as time-dependent strain per unit stress [91]. In addition to temperature, creep compliance varies with the constituent's properties

and their proportion in the asphalt mix. Compacted mix properties like air void also affect creep compliance results, hence, affecting GKM parameters. Since India is a region with a tropical climate and temperature varies from -2^{o} to more than 40^{o} C (approximately) throughout the year [194]; hence, it is important to study mix behaviour at different temperatures. Also, the lack of quality control in mix compaction results in a wide range of air voids. Under these conditions, a lot of uncertainties in the calculation of GKM are expected depending upon region and season. At the end, these uncertainties will result in unreliable design and a significant reduction in their expected lifetime. So, it is important to understand mix behaviour under these conditions.

In this study, the Prony series and power law series have been used to model linear viscoelastic material properties of popularly used bituminous concrete (BC-2 of NMAS 13.2 mm). Power law series is a simple power function of time in which evaluation of only instantaneous creep compliance and time exponent is required [195]. From the computational point of view, a Prony series representation is preferable to a power law model because of its efficiency and better exponential fitting of material response [196]. In the present study, the five-term Prony series and single-term Power series are used to model the viscoelastic properties of BC-2. It is noted that the Power Law series has been kept simple just for the pre-smoothing and comparison purposes only. Pavement response analysis has been carried out based on outcomes of the Prony series model only. The Prony series model was also used to convert creep compliance to relaxation modulus E(t). The interconversion technique is based on an approximate solution developed by Schapery and Park [197]. The flowchart of the methodology and experimental plan for the characterization of asphalt mixes are shown in Figure 3.3.

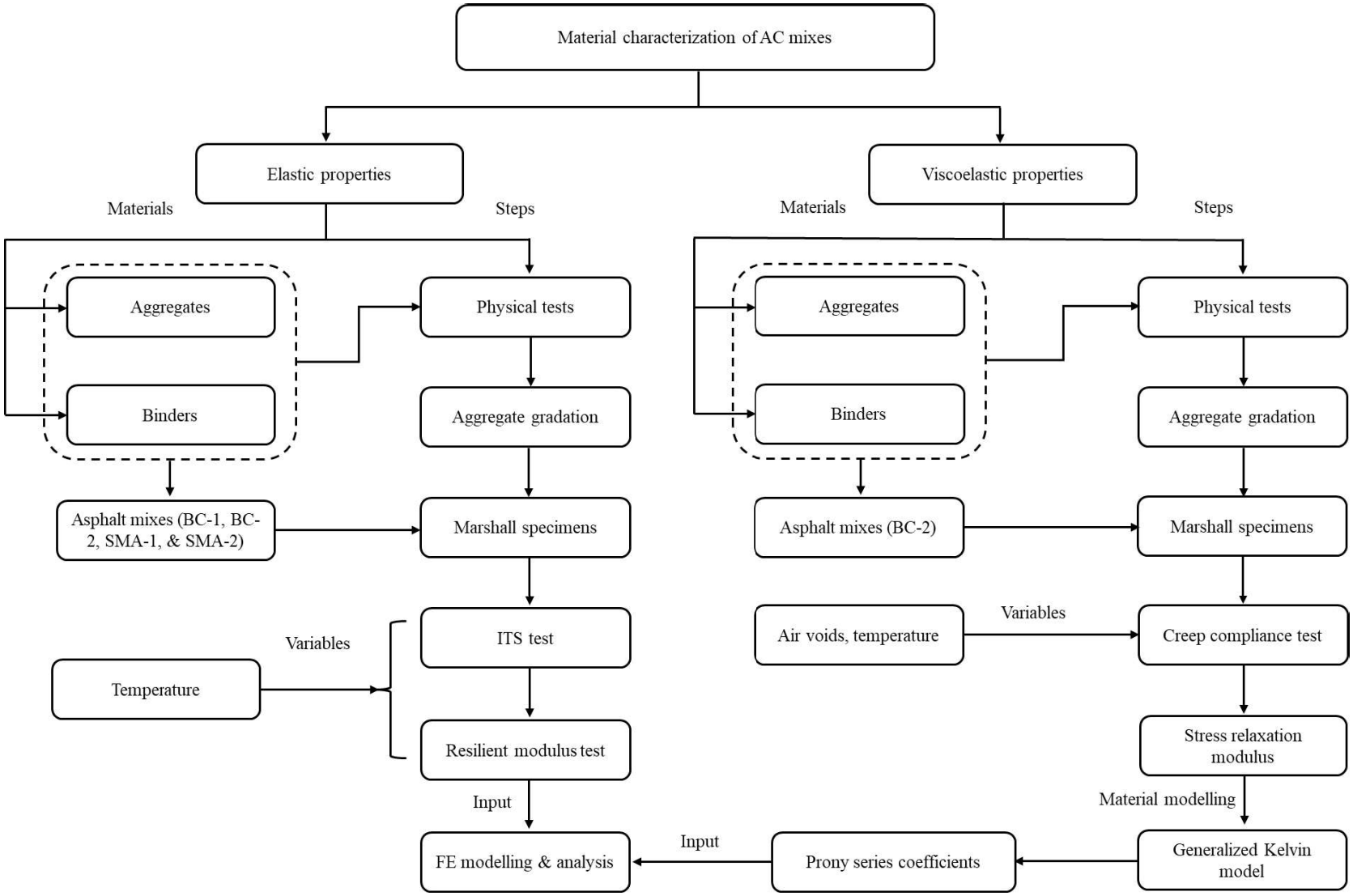

Figure 3.3. Flowchart for the material characterization of asphalt mixes.

3.3 Step II: Nonlinear stress dependent behaviour of unbound granular materials

Material characterization of unbound granular layers (base, subbase, and subgrade) is based on resilient modulus test. The first step involves aggregate gradations for base and subbase layers (soil passing 4.75 mm IS sieve was used for subgrade layer). The selected gradation of aggregates (grade V and VI) for granular subbase layer, WMM, and 4.75 mm passing soil is used to determine the optimum moisture content (OMC) and maximum dry density (MDD) using modified Proctor test. The OMC is used to compact the sample for resilient modulus test.

The cylindrical sample of 100 mm diameter and 200 mm height is used to compact the UGMs at OMC for resilient modulus test. Resilient modulus test was conducted using repeated load triaxial compression testing. The cyclic stress is applied axially whereas confining stress in triaxial chamber is applied through air. Two axial LVDTs are attached to the triaxial compression unit which can measure the axial deformations in the sample. A total of 15 sequence of loading is applied to the sample in which cyclic stress and confining stress are varied in regular interval. The resilient modulus of the UGMs is obtained using deviatoric stress applied to the sample and recoverable strain in the material.

These resilient modulus data as obtained from triaxial compression testing is nonlinear and various stress dependent material models can be used to represent its behaviour. In this study, k-Θ model, Uzan model, and NCHRP model were used for base and subbase layer whereas, Bilinear model was used for subgrade layer. These stress dependent material models were used to evaluate Hypo-elastic material constants considering constant bulk modulus and it was further used as input parameter in the FE model. The flowchart for the material characterization of UGMs are shown in Figure 3.4.

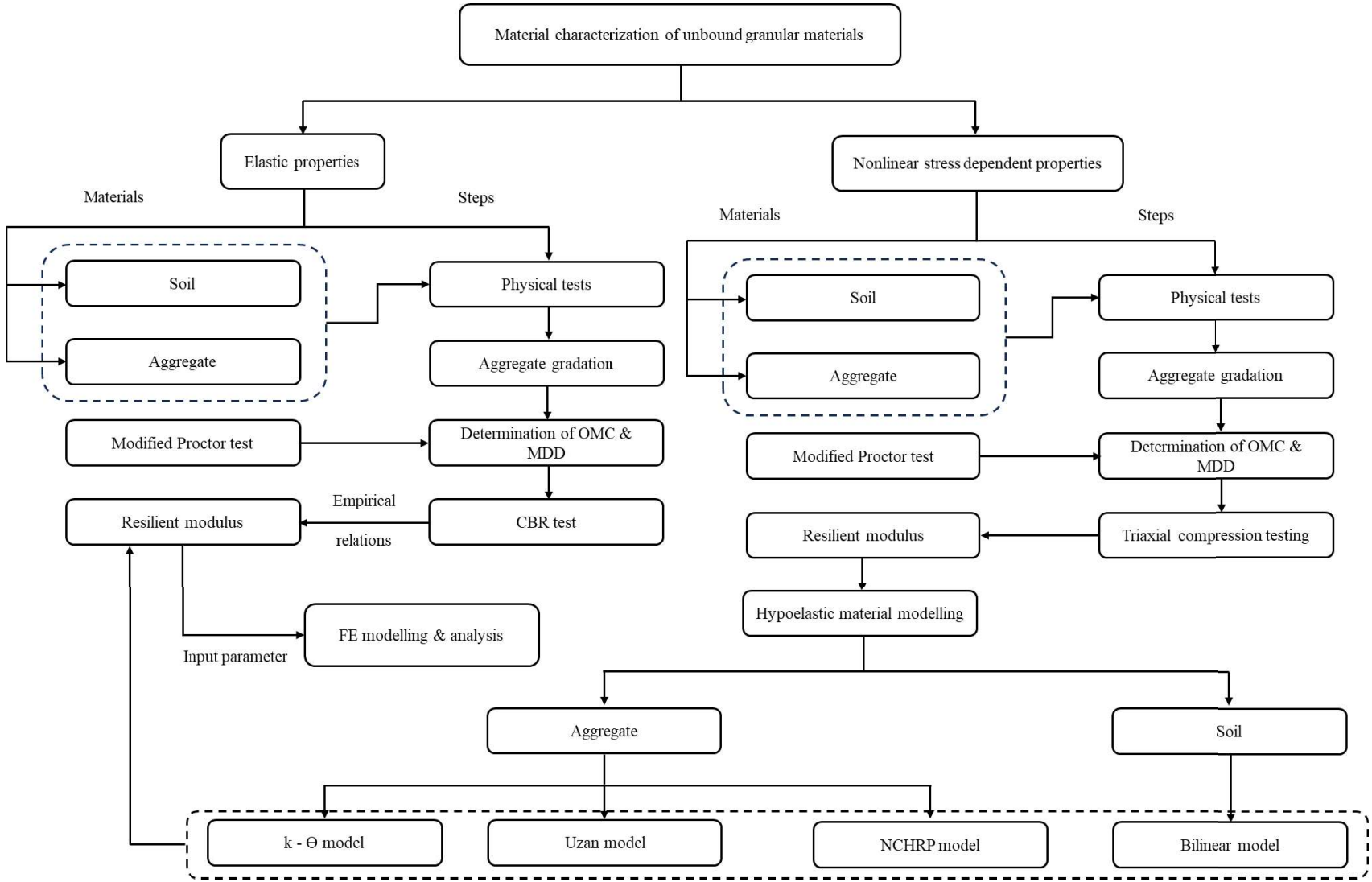

Figure 3.4. Flowchart for the material characterization of UGMs.

The assumption of constant bulk stress could introduce inaccuracies simulating significant stress-dependent volumetric behavior. However, the assumption of constant bulk stress, simplifies the analysis by reducing number of variables. This assumption holds good for representing unbound granular materials response under static loading simulation. Analyzing pavement materials with constant bulk stress requires less computational effort and time compared to more complex, variable stress models (used in "User based Material subroutines"). This efficiency is particularly valuable for conducting multiple simulations for different design scenarios.

3.4 Step III: Finite element modelling of tire-pavement system

Performing research studies in field is generally labour intensive, time-consuming, and expensive. Due to advancements in computational facilities in modern days, properly calibrated FE tools have proven to be a good alternative [198]. In this research, a three-dimensional FE model of tire-pavement system using solid tire and deformable AC pavement was developed. The tire was modelled to consider nonuniform contact stress distribution at the tire-pavement interface. The following subsections present a brief description of the developed FE model.

3.4.1 Finite element modelling of asphalt pavement

A conventional asphalt pavement system with four layers, AC (wearing and binder course), granular base, subbase, and compacted subgrade layer over natural formation was modelled. FE modelling of asphalt pavement was done using ABAQUS which is capable of handling complex material properties of various layers and nonuniform loading. ABAQUS is inbuilt with various modules to define pavement model, material properties, type of analysis, loading, element type, and mesh size. It also facilitates use of nonlinear constitutive equations to represent various material response in the pavement.

The pavement modelling starts with part module in which dimensions of various layers of the asphalt pavement is defined. A pavement of 4 m × 2 m cross section has been modelled in this module. The thickness of asphalt layer (combined thickness of surface and binder course), base layer (wet mix macadam, WMM), granular subbase layer, and subgrade layer has been kept 150 mm, 300 mm, 350 mm, 500 mm respectively. A single drainage cum filter layer of granular subbase has been considered in this study. The natural subgrade (foundation) of 6 m thickness below compacted subgrade layer has been considered as stresses to this depth almost subsides to zero.

The next step is to define the material properties of various layers. It requires material characterization of asphalt mixes and UGMs as discussed later in Chapter 4 and Chapter 5 respectively. Resilient modulus and Poisson's ratio is used as an input parameter in FE modelling considering linear elastic properties of materials. Creep test data (used in this study as discussed in chapter 4) or stress relaxation data in time or frequency domain is used to model linear viscoelastic properties of asphalt mixes in FE model. For defining stress-dependent response of UGMs, either user defined material subroutine or hypo-elastic material modelling based strain invariant parameters can be used. Present study uses strain invariant parameters as discussed later in chapter 5 to characterize UGMs response to cyclic loading.

After defining material properties, various layers are assembled together in assembly module. Layers are kept in contact to each other using linear translation or rotation of various instances. In the next step, type of analysis (static or dynamic), number of time increments, equation solver (direct or iterative), and solution technique (full Newton, quasi-Newton etc.) is defined in the "Step" module. Present study considers static loading condition. The interaction between pavement layers is defined in the next step using surface to surface contact (used in present study), standard contact, or elastic foundation.

The Penalty friction formulation has been selected to define tangential contact property at the interface of the layers. It makes the simulation more realistic. The friction coefficient at the interface of the various layers has been determined using Newton's inclined plane test. In this test, sample specimen of unbound granular layers is compacted at maximum dry density and optimum moisture content while asphalt samples are compacted at design air void. The one sample is placed over other (in order as they are laid in field during pavement construction) and the inclination of sample placed in lower position is keep on increasing till the moment sample placed over it just starts sliding. This inclination is noted and tangent of it is recorded as friction coefficient at the interface. The details of measured friction coefficient at the interface of various layers have been shown in Table 3.1.

Table 3.1. Friction coefficients at the interface of pavement layers

Surface in contact	**Sliding angle**	**Friction coefficient**
Asphalt concrete – conventional	33.82^o	0.67
Asphalt concrete – stabilized base	31.38^o	0.61
Conventional base - subbase	35.75^o	0.72
Stabilized base – subbase	32.21^o	0.63
Subbase - subgrade	27.47^o	0.52

The hard contact (fully bonded) as normal behaviour was defined under the interaction module. The layer of higher stiffness was assigned master surface while layer with lower stiffness as slave surface.

In the next step, loading and boundary conditions were defined. The axle loading has been simulated using real tire body discussed in later section. The static loading condition has been simulated in present study and magnitude of loading is assigned to the reference node created at the centre of tire body. Although, the field loading conditions can be better

represented considering dynamic loading simulations. However, static loading simplifies the analysis process by assuming that the loads are applied slowly enough that inertial effects (acceleration) can be neglected. This makes the problem easier to solve and reduces computational complexity. Static analysis generally requires less computational effort and time compared to dynamic analysis. This is because dynamic analysis involves solving equations of motion, which can be more complex and computationally intensive. The analysis time for a single run, considering static loading conditions was approximately 3 hours and 24 minutes using a system with core i7-10750H CPU, 16 GB RAM, 6 cores, and 2.60 GHz processor speed. Dynamic simulations, require high speed computers (parallel computing techniques, like supercomputer) for running complex tire-pavement interaction models. However, we will be definitely considering dynamic simulations in our future studies. The boundary conditions used in this study has been discussed separately in later section.

The final step before the solver runs for solving system of equilibrium equations for obtaining structural response of the asphalt pavement is meshing. In this module, pavement layers and tire are meshed into several parts to generate number of elements and nodes in the structure. Meshing discretizes complex geometries into a set of simple and interconnected elements.

3.4.2 FE modelling of solid tire

The current design method of AC pavement assumes a circular contact area and uniform distribution of vehicle load, which could significantly differ from the actual field conditions [161,162]. The assumption is used because it simplifies the calculation in pavement analysis. However, it is difficult to explain the behaviour of distresses in AC pavement gradually developing from the surface under heavy vehicles using a simple

uniform loading in FE analysis [161], [163–165]. Therefore, it is necessary to consider nonuniform contact stress distribution in the FE model. A 3-dimensional test tire was modelled to simulate the complex stress distribution over the loading area. Solid tire in India is generally used in forklift trucks and construction equipment. Solid tires are more popular in heavy-duty vehicles due to their ability to withstand excessive loads and operational capability in harsh environments [167]. It is also easy to evaluate the material properties of solid tire as it consists of single rubber material. For modelling tire rubber, the suitable hyper-elastic material model was obtained using relevant tensile test data and a curve fitting approach [168]. Hyper-elastic models are generally used to calculate elastomer's properties that respond elastically when subjected to large deformations [169]. These material models are expressed in the form of polynomial functions. The generalized strain energy density function for incompressible materials is explained as shown in Eq. 3.1 below.

$$U = U(F) - P(J - 1) \tag{3.1}$$

where J is determinant of the deformation gradient matrix and U(F) can be expressed as shown in Eq. 3.2:

$$U(F) = U(I_1, I_2, I_3) = U(\lambda_1, \lambda_2, \lambda_3) \tag{3.2}$$

where $I_1, I_2, and\ I_3$ are the first, second, and third strain invariant and $\lambda_1, \lambda_2, and\ \lambda_3$ are the primary elongation [199]. The Yeoh hyper-elastic material model was selected using the curve fitting method to describe the mechanical behaviour of test tire rubber. The constitutive Yeoh model for compressible rubber is presented in Eq. 3.3.

$$W = \sum_{i=0}^{3} C_{10}(\overline{I_1} - 3)^i \tag{3.3}$$

where W is the strain energy density function, $\overline{I_1}$ is the first principal invariant and C_{10} is the material constant. The material constant C_{10} is interpreted as half the initial shear modulus. Table 3.2 shows the material model constants used in the analysis.

Table 3.2. Coefficients of material model for solid tire

Material	**Coefficients (MPa)**		
Rubber	C_{10}	C_{20}	C_{30}
	0.684	-0.022	0.007

3.4.3 FE modelling of tire-pavement interaction

In this research, the developed model uses contact approaches as proposed by previous researchers [200,201]. As a first step, the contact between the two interacting surfaces of tire-pavement bodies is defined [202]. Both the surfaces (tire and pavement) are considered as deformable, the tire being considered a slave surface whereas the pavement surface was considered a master surface. A finer mesh in the tire region was considered as nodes on the slave surface were not allowed to penetrate the master surface. The interfacial contact was defined using the Penalty function (see Eq. 3.4) and a tangential contact was defined using the Coulomb friction model as shown in Eq. 3.5. More details about the contact formulation can be found elsewhere [203].

$$F_n = \begin{cases} S_n C & C \leq 0 \\ 0 & C > 0 \end{cases} \tag{3.4}$$

$$F_t = S_t \delta^e \tag{3.5}$$

where F_n is the normal interaction force, F_t is tangential interaction force, S_n and S_t are normal and tangential contact stiffness respectively, C is the clearance value of the node in contact relative to the target surface, and δ^e represents elastic deformation of the contact node relative to the target surface.

3.4.4 Description of element type and boundary conditions

Pavement depth is considered to be 6 m in vertical direction (-z) to represent the semi-infinite layer below the compacted subgrade as shown in Figure 3.5. The pavement layers need to be meshed, allowing complex geometry to be divided into smaller, simpler geometric elements. It enables the numerical solution of complex pavement model by approximating the continuous behavior of various layers with a discrete set of points (node sets) and equations across each element, leading to more accurate simulation results. The choice of element type depends on complexity of geometry, material behavior, accuracy, and computational cost.

A tetrahedral mesh extends the concept of a 2D triangular mesh into three dimensions. Tetrahedral elements are often created as equilateral, especially in systems with circular curvature, or as isosceles tetrahedra in asymmetric systems. These elements can also be entirely unstructured, allowing them to adapt to complex geometries with high precision. This precision surpasses that of a simple cubic grid in 3D or a square grid in 2D.

A hexahedral mesh extends the idea of a 2D quadrilateral mesh into three dimensions, but it doesn't always follow a cubic (Cartesian) point arrangement. A hexahedral mesh offers the flexibility to approximate curves or bends in flat surfaces by adjusting the angles between quadrilateral faces along the mesh. A hexahedral mesh can capture the flat surface having curved edge with perfect accuracy, allowing for lower node and element

density along that surface. In the curved region, node density can be increased to capture flows along that specific surface with higher accuracy.

This demonstrates the advantages of hexahedral meshes over tetrahedral elements for certain types of flows with small curvature. Additionally, computation time can be reduced in some systems because the total element count can be lower than with a tetrahedral mesh.

Considering these advantages, the 8-node hexahedral brick element was used to model pavement layers. A higher number of elements (fine meshing) closer to the loading area and a lesser number of elements (relatively coarser mesh) away from the loading area were considered as shown in Figure 3.5. The friction coefficient between pavement surface and tire is kept 0.35 as considered in past studies [204]. The element size in AC layer closer to loading area is kept 30 mm × 30 mm while it is 70 mm × 100 mm away from the loading area. In lower layers of the pavement, element size is kept 30 mm × 100 mm closer to loading area while 70 mm × 100 mm away from the loading area. The element size of the outer surface of solid tire is kept 15 mm × 15 mm in this study.
To simulate realistic field constraints, elements in the longitudinal direction (4 m) of AC pavement were kept free to move. The elements in the transverse direction (2 m) were constrained (fixed boundary) as it is supported by the shoulder area. Movement of all the nodes in the vertically downward direction was allowed. The bottom elements of natural foundation were fixed in all degrees of freedom as stress to this depth generally subsides to zero. After defining element types and boundary conditions to the FE model, the problem was submitted for the evaluation of pavement response under job module. Figure 3.5 shows the FE model of tire-pavement system.

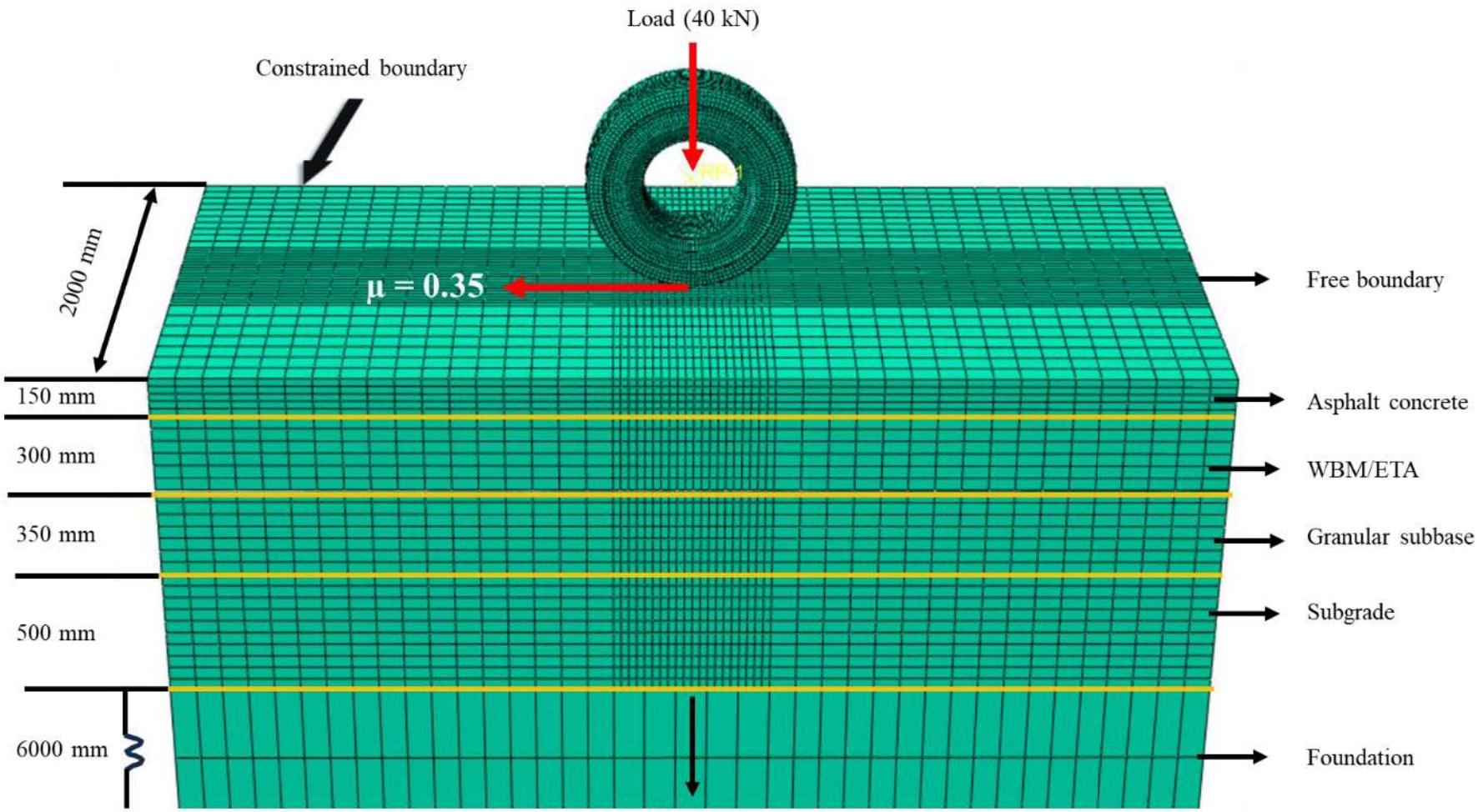

Figure 3.5. FE model of tire-pavement system.

3.5 Validation of FE model

To check the accuracy, the FE model of tire-pavement system was validated using responses obtained from 3D Move Analysis [205] software. The contact area corresponding to different tire loads and maximum vertical deformations in the AC layer were selected as response criteria. The FE simulations were carried out considering BC-2 mix (E = 3000 MPa and υ = 0.35) with a conventional base (WMM) layer with the identical input parameters of 3D Move Analysis [205]. The considered material properties of unbound granular layers were obtained from laboratory testing as shown in Table 3.3.

Table 3.3. Material properties of unbound granular layers

S No.	Pavement layers	Thickness (mm)	CBR (%)	M_r (MPa)	υ
1	Subgrade layer	500	10.80	80	0.35
2	Subbase layer	350	N.A.	295	0.35
3	Base layer	300	N.A.	295	0.35

N.A. = Not applicable

The method of determination of these properties are explained in detail in chapter 4 and 5 respectively. Here, these experimental data have been presented for the reference of readers as it has been used in the validation of FE model. Figure 3.6 shows a comparison of the predicted contact area and maximum AC deformations under different loading levels for the proposed FE model and 3D Move analysis.

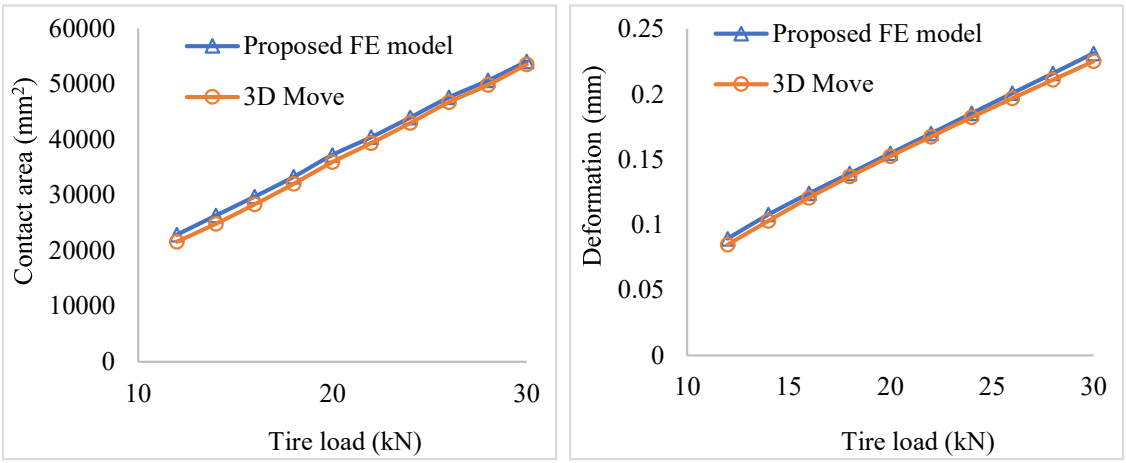

(a) (b)

Figure 3.6. Variation of (a) contact area and (b) maximum deformation in AC layer with different tire loads.

As shown in Figure 3.6, a good agreement was found between the results obtained from 3D Move Analysis and the proposed FE model. A maximum difference of 5.87% in the estimated contact area from the two methods as shown in Figure 3.6 (a) was found. As shown in Figure 3.6 (b), a maximum difference of 5.37% in maximum vertical deformation was found. The average difference in contact area was found to be 3.39% while 2.61% for maximum deformation. Considering the apparent difference between FE and 3D Move software, the difference can be taken as relatively small.

The variation of vertical compressive stress (σ_v) against pavement depth as obtained from FE and 3D Move analysis are also plotted as shown in Figure 3.7. The analysis is done for 40 kN wheel load and standard pressure of 0.56 MPa, keeping material properties and other parameters same as discussed in previous paragraph for evaluating contact area and maximum deformation in AC layer by the two approaches.

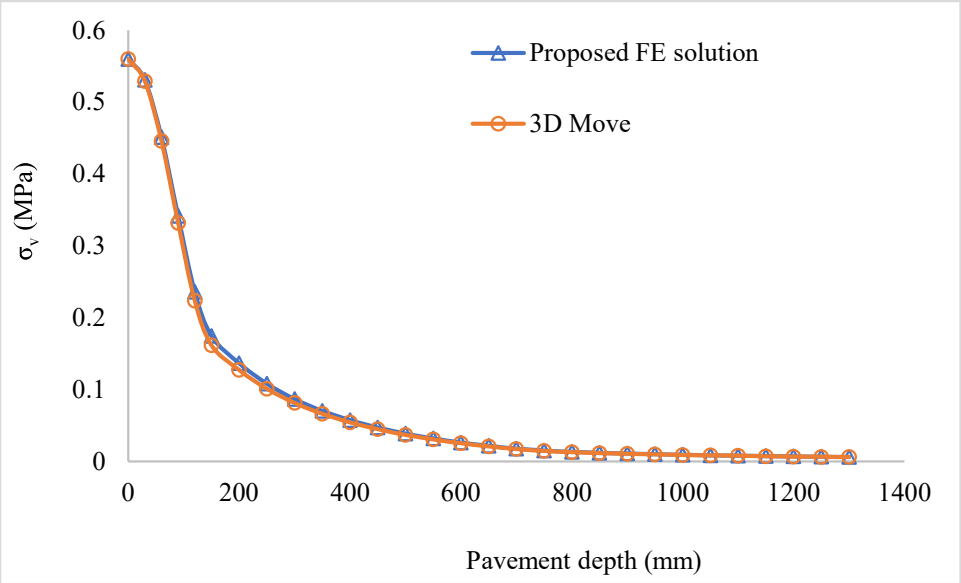

Figure 3.7. Comparison of proposed FE solution and 3D Move solution.

As shown in Figure 3.7, vertical compressive stress obtained from FE solution and 3D Move analysis were found in good agreement throughout the depth of the pavement. The average difference in σ_v between the two methods was found to be 3.78%. It can be concluded that the proposed FE model predicts structural response of the asphalt pavement reasonably well and can be used further for pavement analysis.

The developed FE model was also validated with Boussinesq closed-form analytical solution (see Eq. 3.6), which is used for uniform circular pressure [127]. Boussinesq's solution is used to calculate vertical stress at any depth in the soil due to point load. It assumes soil as elastic, homogeneous, and isotropic. To simulate the identical condition, all the layers were assigned the same elastic modulus (100 MPa), and Poisson's ratio (0.4), transforming the four-layer system into a single layer. A single wheel load having a uniform pressure of 560 kPa over a circular area of 110 mm radius was considered for the analysis. A comparison between vertical compressive stress (σ_v) obtained using the Boussinesq solution–and FE analysis is shown in Figure 3.8. As can be seen in the corresponding figure, a good agreement between the FE model and analytical solution was found.

$$\sigma_v = p\left(1 - \frac{1}{\left(1 + \left(\frac{r}{z}\right)^2\right)^{\frac{3}{2}}}\right) \tag{3.6}$$

where p is uniform pressure, r is the radial distance from the point load, and z is the depth at which vertical stress is calculated.

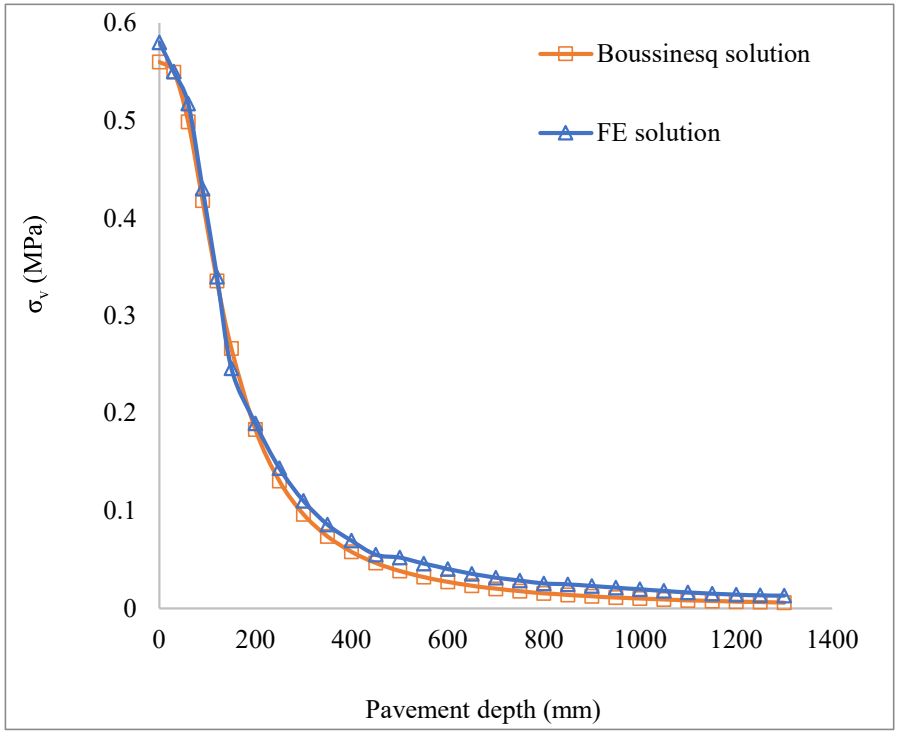

Figure 3.8. Comparison of Boussinesq close form and FE solution.

As shown in Figure 3.8, it was found that, solutions obtained from Boussinesq close form equation and FE analysis were in close agreement for top 200 mm depth of the pavement and average difference in σ_v from the two analyses were 2.18% only. However, with the further increase in depth, Boussinesq solution provides lower σ_v (σ_v was found 64% lower at the top of the subgrade) compared to FE analyses. The difference in computed σ_v by the two approach tends to increase at higher depths due to several factors. The Boussinesq solution underestimates the stresses at higher depths. The self-weight of the material is ignored, and the vertical stresses are independent of the elastic modulus and Poisson's ratio of the material in Boussinesq solution. The vertical stress decreases rapidly with an

increase in r/z ratio. Actually, at r/z = 5 or more, stress calculated using Boussinesq solution is extremely small and negligible. Additionally, the Boussinesq solution does not consider the finite extent of pavement layer, which is more pronounced at higher depths. Additionally, FE method uses numerical methods to solve the governing equations for each element, providing precise calculation of stress distribution. The precision becomes more significant at higher depths, where small difference in load distribution has larger impact on σ_v values. So, results obtained from FE analysis is considered more reliable.

3.6 Step IV: Parametric analysis and structural response of asphalt pavement

The final step consists of parametric analysis of the asphalt pavement using developed FE model considering various parameters actually affecting the structural response of the pavement. These parameters include material properties of asphalt mixes (linear and viscoelastic), UGMs (elastic and nonlinear stress dependent), loading conditions (using real tire), climatic conditions (temperature), base layer stabilization, layer thickness etc. Effect of these parameters on the structural response of asphalt pavement and change in pavement life in rutting and fatigue has been discussed in detail in Chapter 6.

3.7 Summary

This chapter discusses experimental plans for testing asphalt mixes and UGMs and FE modelling of tire-pavement system. The methodology of linear elastic and linear viscoelastic characterization of asphalt mixes has been highlighted in step I. The linear elastic properties of mixes are based on resilient modulus test. Poisson's ratio has been taken from IRC:37 for all the mixes. The linear viscoelastic characterization of asphalt mixes is based on creep compliance test. These creep data have been further converted to stress relaxation data using approximate methods. The generalized Kelvin model has been

used to fit these stress relaxation data and Prony series coefficients have been determined to be used as an input parameter in FE method.

The experimental plan for evaluating linear elastic and stress dependent response of UGMs has been discussed in the next step (step II). The linear elastic properties of UGMs are based on resilient modulus and Poisson's ratio. The resilient modulus has been obtained from empirical relations as specified in IRC:37 based on CBR test data and Poisson's ratio as suggested in this design code. The stress dependent response of UGMs is based on repeated load triaxial compression testing and hypo-elastic modelling of strain invariant parameters.

The last section highlights FE modelling of asphalt pavement system which has been further used for the parametric analysis. It briefly explains, FE modelling of 3-dimensional asphalt pavement system, solid tire using hyperelastic modelling of tire rubber, tire-pavement interaction, element types, and boundary conditions used in this study for pavement analysis. The FE model can handle the complex material properties of various layers in the asphalt pavement.

The material characterization of asphalt mixes and UGMs are required to define layer stiffness under property module in the FE model. These properties form the basis of layer strength and its resistance to loading. For this purpose, experimental determination of resilient modulus and creep compliance of asphalt mixes have been discussed in chapter 4. The linear viscoelastic simulation and determination of Prony series coefficients has also been highlighted. While the material stiffness of UGMs based on soil CBR values and stress dependent behaviour based on repeated load triaxial testing has been discussed in chapter 5. This chapter also highlights the suitability of various stress dependent

resilient modulus models like k-θ, Uzan, NCHRP (octahedral shear stress model), and Bilinear model for aggregate and soil material.